Investigation on temperature characteristics of weak fiber Bragg gratings in a wide range

Xiaojun Fan (樊晓军)[1,2,3], Junfeng Jiang (江俊峰)[1,2,3,*], Xuezhi Zhang (张学智)[1,2,3,], Kun Liu (刘 琨)[1,2,3], Shuang Wang (王 双)[1,2,3], and Tiegen Liu (刘铁根)[1,2,3]**

[1]*School of Precision Instrument and Opto-electronics Engineering, Tianjin University, Tianjin 300072, China*

[2]*Tianjin Optical Fiber Sensing Engineering Center, Institute of Optical Fiber Sensing of Tianjin University, Tianjin 300072, China*

[3]*Key Laboratory of Opto-electronics Information Technology, Ministry of Education, Tianjin University, Tianjin 300072, China*

**Corresponding author: jiangjfjxu@tju.edu.cn; **corresponding author: zhangxz@tju.edu.cn*

Received June 22, 2019; accepted August 22, 2019; posted online December 2, 2019

A weak fiber Bragg grating (WFBG) is an ideal quasi-distributed optical fiber sensor. Special attention should be paid to the spectrum and sensing performance of the WFBG at extreme temperatures due to its poor reflection intensity. In this Letter, the temperature characteristics of the WFBG from −252.75°C to 200.94°C are experimentally investigated. Five WFBGs with reflectivity from ~0.25% to ~10% are used in the experiments. The reflectivity variations and wavelength shifts at different temperatures are studied. Experimental results show that the WFBG can survive and work at extreme temperatures, but the performance is affected significantly. The reflectivity is affected significantly by both cryogenic temperature and high temperature. The temperature responses of Bragg wavelengths in the wide temperature range are also obtained.

OCIS codes: 060.3735, 060.2370, 230.1480.

doi: 10.3788/COL201917.120603.

Fiber Bragg grating (FBG)-based sensors have been widely used in many fields due to the advantages of small size, flexibility, ease of embedment into a structure, and immunity to electromagnetic fields[1,2]. Extreme-temperature-resistant FBGs have also been systematically studied for years[3–5]. In applications where measurements of dense points are required, such as structural health monitoring[6], a large number of FBGs are distributed over the entire sensing area. However, the maximum multiplexing capacity of FBG sensor arrays is limited, although various multiplexing methods are used, e.g., wavelength-division multiplexing, time-division multiplexing, and so on[7,8]. Recently, the weak FBG (WFBG) has attracted wide attention because of its extremely low reflectivity, which will reduce the crosstalk between multiple gratings and, hence, greatly increase the multiplexing capacity of the sensor array on a single length of optical fiber[9–11]. Such large-scale WFBG sensor arrays combined with optical frequency domain reflectometry and optical time domain reflectometry have been one of the hottest research topics in recent years[12].

Even though a WFBG is an ideal quasi-distributed sensor, its temperature characteristics have not been systematically studied. For the engineering structures designed to operate at cryogenic temperature or high temperature, such as liquid hydrogen (LH_2) fuel tanks employed in aerospace vehicles[13], storage or transport vessels for cryogens[14], and fossil fueled steam power plant[15], the reliability and accuracy of sensors at extreme temperatures are required. For traditional FBGs with high reflectivity (usually greater than 80%), only accurate monitoring of the Bragg wavelength is needed, without paying special attention to the reflection intensity. However, for WFBG with low signal-to-noise ratio (SNR) of the reflection spectrum, the influence of temperature cannot be ignored. An extreme temperature environment may lead to a decrease of the reflection intensity and even the failure of peak detection.

In this Letter, we experimentally investigate the temperature characteristics of the WFBG from −252.75°C to 200.94°C. The WFBGs with reflectivity from ~0.25% to ~10% are used and encapsulated with a capillary glass tube to avoid errors caused by gas flow and liquid flow. The reflectivity at extreme temperatures is studied, and the wavelength shifts from −252.75°C to 200.94°C are obtained.

The mechanism of a Bragg grating can be understood and modeled by several approaches[16–18]. As for the uniform Bragg grating with less index perturbation, coupled-mode theory has higher precision. In the general case, the index perturbation $\delta n(z)$ takes the form of a phase and amplitude-modulated periodic waveform:

$$\delta n(z) = \delta n_{\mathrm{core}} + \delta n_0(z)\left\{1 + v\cos\left[\frac{2\pi z}{\Lambda(z)} + \Phi(z)\right]\right\}, \quad (1)$$

where δn_{core} is the refractive index of the core, $\Phi(z)$ is the phase, $\Lambda(z)$ is the grating period, and the fringe visibility of the refractive index is given by the parameter v, which is determined by the visibility of the ultraviolet (UV) fringe pattern. The effective index is $n_{\mathrm{eff}} = \delta n_{\mathrm{core}} + \delta n$.

The characteristics of the reflection spectrum are given as follows.

The Bragg wavelength is

$$\lambda_B = 2n_{\mathrm{eff}}\Lambda(z), \tag{2}$$

and the reflectivity is

$$R = \frac{\sinh^2(\sqrt{\kappa^2-\sigma_0^2}L)}{\cosh^2(\sqrt{\kappa^2-\sigma_0^2}L)-\sigma_0^2/\kappa^2}, \tag{3}$$

where L is the length of the grating, κ is the AC coupling coefficient, and σ_0 is the DC coupling coefficient, which is related to mode detuning σ. For a single-mode fiber grating, the coupling coefficients are given by

$$\kappa = \frac{\pi}{\lambda}\nu\delta n, \tag{4}$$

$$\sigma = \frac{2\pi}{\lambda}\delta n. \tag{5}$$

From Eqs. (2)–(5), the Bragg wavelength and reflectivity are all related to the refractive index, while the refractive index is affected by ambient temperature. However, it is difficult to get analytical expressions because of the complexity of numerical calculation. Therefore, it is necessary to experimentally study the temperature characteristic of WFBGs at different temperatures.

The WFBGs used in this study are manufactured in our laboratory using the phase mask method[19]. Photosensitive fiber (Fibercore PS750) with a dopant of boron, numerical aperture of 0.12, core diameter of 9 μm, and attenuation of 60 dB/km is chosen in the experiment. The fiber is illuminated using a KrF excimer laser (Coherent BraggStar) at 248 nm, after which the gratings are annealed at 150°C for 8 h to stabilize their performance. The customized reflectivity is achieved by adjusting the laser intensity and exposure time. Five WFBGs with reflectivity of ~0.25%, ~0.5%, ~1%, ~5%, and ~10% are obtained. The reflection spectra are shown in Fig. 1(a).

The experiments are performed in a wide temperature range provided by several devices, including LH_2, liquid nitrogen (LN_2), an alcohol tank, an oven, and an oil bath. The wavelength shift and reflectivity variation at cryogenic temperatures are analyzed in the LH_2 experiment. The long-term stability of the wavelength is analyzed in the LN_2 experiment. The reflectivity variation at high temperature is analyzed in the oil bath experiment. To avoid the errors caused by gas flow and liquid flow, the WFBG is encapsulated by capillary quartz tube with a diameter of 300 μm, as shown in Fig. 1(b). All of the capillary encapsulated WFBGs are mounted in close thermal contact with a calibrated platinum resistance thermometer (PRT, Fluke5609). The preset temperature in different devices and the actual temperature measured by the PRT are given in Table 1. All of the values are recorded after the device is fully stabilized. The spectra and Bragg wavelengths of the WFBGs are recorded by a self-developed Fabry–Perot filter-based demodulator[20].

The LH_2 experiment is conducted firstly in a dewar similar to the device used in previous thermal expansion measurements[21]. An acrylate coated WFBG with reflectivity of ~0.25% is used as a comparative experiment to investigate the effect of the coating. The coated WFBG is also encapsulated in a capillary quartz tube and mounted with the PRT. Then, the PRT and WFBGs are slowly immersed in LH_2 and experience cryogenic temperatures for about 15 min. Figure 2(a) shows the wavelength shifts of the coated and bare WFBGs with reflectivity of ~0.25% during the experiment. As expected, the wavelengths are plunged when the WFBGs are immersed in LH_2 and restored when the WFBGs are taken out from LH_2. However, the wavelength shift of the coated WFBG is significantly greater than that of the bare WFBG. It is because the high thermal expansion coefficient of the acrylate

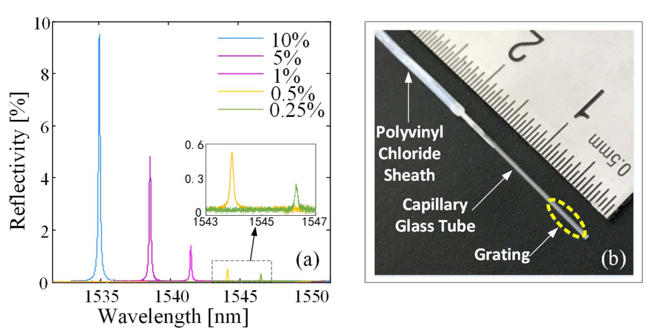

Fig. 1. (a) Reflection spectra of WFBGs with reflectivity of ~0.25%, ~0.5%, ~1%, ~5%, and ~10%. Inset: the reflection spectra of 0.5% and 0.25% reflectivity WFBGs. (b) Photograph of a WFBG encapsulated by a capillary quartz tube.

Table 1. Ambient Temperatures of Different Devices

Device	Preset Temperature (°C)	Actual Temperature (°C)
LH_2	–	−252.75
LN_2	–	−195.43
Alcohol tank	−80	−80.06
Alcohol tank	−60	−59.71
Oven	−40	−39.62
Oven	−10	9.42
Oven	20	19.75
Oven	50	49.06
Oven	80	79.03
Oven	110	107.75
Oven	140	135.10
Oil bath	170	170.27
Oil bath	200	200.94

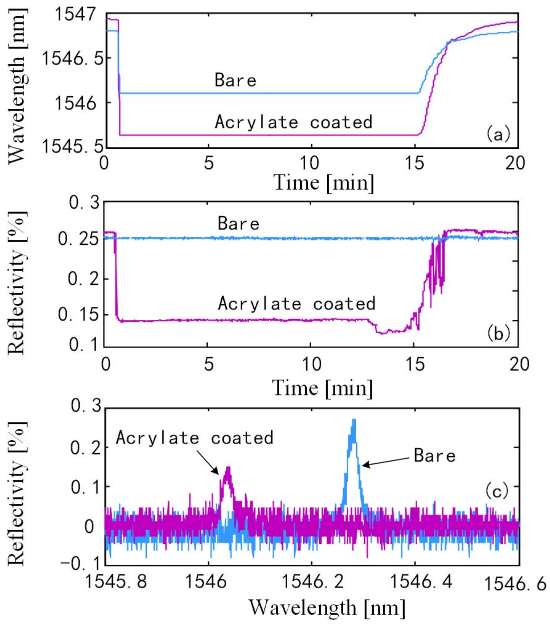

Fig. 2. (a) Wavelength, (b) reflectivity, and (c) reflection spectra of WFBGs with reflectivity of ~0.25% in LH_2 immersion experiments.

coating improves the temperature sensitivity of WFBG at cryogenic temperatures.

The reflectivity variations of the acrylate coated and bare WFBGs are shown in Fig. 2(b). The reflectivity of the bare WFBG is stable from room temperature to −252.75°C, which is consistent with the result in Ref. [22]. However, the reflectivity of the coated WFBG is decreased instantaneously from ~0.25% to ~0.15%, corresponding to a ~40% drop. The decrease may also be related to the thermal expansion of acrylate coating. The thermal expansion of the coating layer causes uneven stress in the grating region, affecting the refractive index and period of the grating, resulting in a decrease in reflectivity. Figure 2(c) shows the reflection spectra of the WFBGs immersed in LH_2. It can be seen from the figure that the decrease in the reflectivity of coated WFBG results in a poor reflection intensity, which is difficult for accurate peak detection. The coated WFBGs with higher reflectivity show similar results. The reflectivity of the bare WFBG is not affected by temperature, whereas that of an acrylate coated WFBG will decrease to some extent in LH_2: ~0.5% decreases to ~0.36% with a 28% reduction, ~1% decreases to ~0.8% with a 20% reduction, ~5% decreases to ~4.4% with a 12% reduction, and ~10% decreases to ~8.9% with a 11% reduction. Therefore, the WFBG with acrylate coating is not suitable for cryogenic temperature applications. In the following experiments, a bare WFBG with capillary quartz tube encapsulation is used.

In the LN_2 experiment, the WFBGs mounted with the PRT are lowered in a LN_2 tank. The immersion lasts for 150 h to validate the long-term stability of reflectivity at cryogenic temperatures. After that, the LN_2 evaporates gradually, and the temperature returns to room temperature. Figure 3(a) shows the real-time temperature during the experiment measured by PRT. The reflectivity variations of the WFBGs with different reflectivity are given from Fig. 3(b) to Fig. 3(f). It is obvious that the reflectivity of all WFBGs remains stable during the experiment. The results indicate that the WFBG can maintain a stable performance at cryogenic temperatures over the long term.

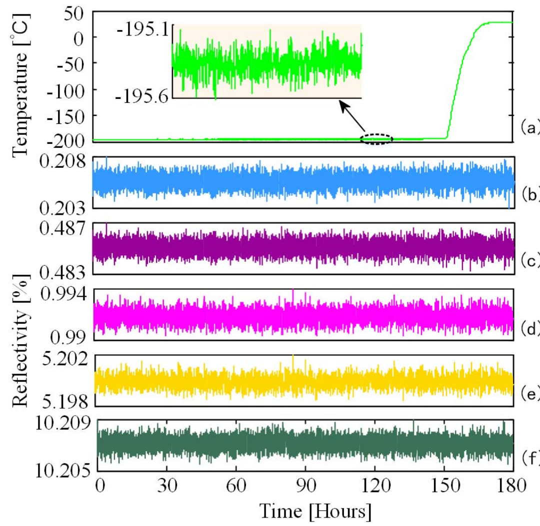

Fig. 3. (a) Temperature during LN_2 experiment; the reflectivity of five WFBGs with reflectivity of (b) ~0.25%, (c) ~0.5%, (d) ~1%, (e) ~5%, and (f) ~10%.

It is well known that the grating erasure at high temperatures will cause the reflectivity to decrease or even disappear. Here, the high temperature experiment is carried out in an oil bath (Demei, DY-HTS300) filled with silicone oil at 170°C. The encapsulated WFBGs are loaded in a sealed glass test tube to avoid direct contact with the silicone oil. The glass test tube is immersed in silicone oil at time t_1, and taken out at time t_2. A few minutes later, the entire assembly is immersed in the oil bath again at time t_3. Then, the silicone oil is heated from 170°C to 200°C. Finally, the WFBGs and PRT are taken out at time t_4. Figure 4(a) shows the temperature measured by the PRT during the experiment. It should be emphasized that at time t_2, the sealed glass test tube containing the WFBGs and PRT is taken out from the oil bath as a whole, so the temperature in the sealed glass test tube decreases slowly. However, at time t_4, the WFBGs and PRT are taken out from the glass test tube directly; therefore, the temperature at time t_4 is decreased significantly faster than that at time t_2.

Figure 4(b) shows the reflectivity variations of the WFBG with reflectivity of ~0.25% during the experiment. As can be seen from Fig. 4, there is a clear correspondence between the reflectivity and ambient temperature. The sudden temperature change results in a decrease in the reflectivity, regardless of whether the temperature is going up or down. The reflectivity decreases at time t_1, t_2, t_3, and t_4. The decreases at times t_1 and t_4 are significantly

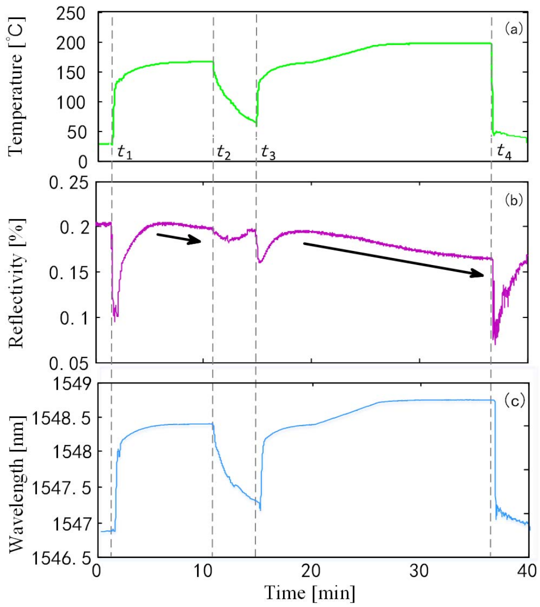

Fig. 4. (a) Temperature, (b) reflectivity variation, and (c) wavelength shift of the WFBG with reflectivity of ~0.25% in silicone oil.

sharper than those at times t_2 and t_3, corresponding to the rapid temperature changes at times t_1 and t_4. A few minutes later, as the ambient temperature is stable, the reflectivity is rebounded. The authors do not find out the sources of the reflectivity decrease. A link to the change of index perturbation $\delta n(z)$ of the grating region was presumed but not yet confirmed. In addition, as indicated by the green arrows in Fig. 4(b), the reflectivity is also gradually decreased in the high temperature environment. The reduction is caused by the grating erasure at high temperatures, which is irreversible[23]. The wavelength shift is also shown in Fig. 4(c), which is consistent with the temperature change.

It should be noted that when the sealed glass test tube is placed in the high temperature oil bath, the air in the test tube is compressed, and the pressure is increased, which may cause an unexpected strain on the WFBG. Therefore, further experiment is designed to verify the effect of sudden strain on reflectivity. The WFBG is pasted on an equal strength cantilever beam. The strain is changed by different weight. It can be seen from Fig. 5 that the reflectivity remains stable as the strain changes. Therefore, the reflectivity decrease in the oil tank experiment is independent of the strain caused by air compression.

Finally, the relationships between the temperature and Bragg wavelength of the WFBGs with different reflectivity are obtained from −252.75°C to 200.94°C. Figure 6 shows the curves of two cycles of heating and cooling. The temperature sensitivities of WFBGs with different reflectivity agree well with each other. The wavelength shifts show good linearity when the temperature is higher than −40°C. As the temperature reduces, the sensitivity decreases too. The temperature responses agree well with previous studies of traditional FBGs[24].

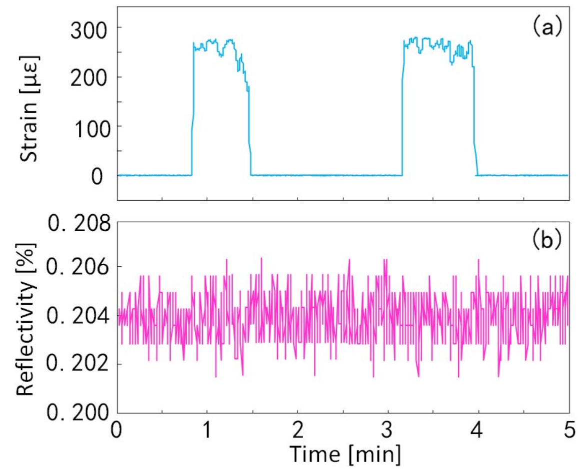

Fig. 5. Strain test results: (a) strain change, (b) reflectivity variation.

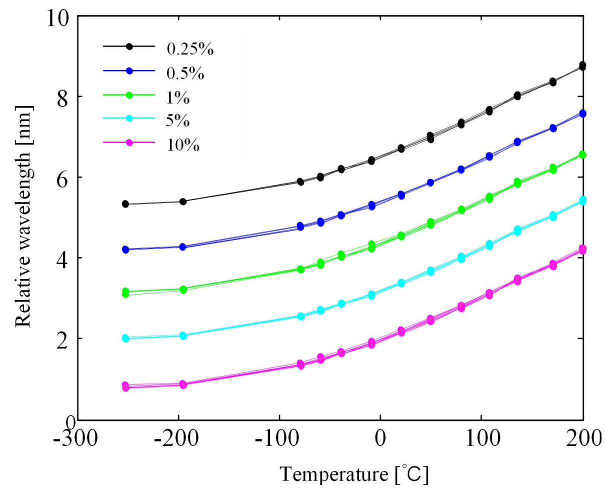

Fig. 6. Wavelength shifts of WFBGs with different reflectivity from −252.75°C to 200.94°C.

According to the above experimental results, the wavelength of the WFBG varies with temperature in the range of −40°C to 200°C, which can be used for temperature measurement. However, the reflectivity may decrease in high temperature and cryogenic temperature environments. Therefore, the reflection intensity and SNR of the reflection spectrum, which are related to the intensity of light source, attenuation of optical path, etc., should be taken into consideration in the applications at extreme temperatures.

In conclusion, the investigations of WFBG temperature characteristics are conducted in the range of −252.75°C to 200.94°C using LH_2, LN_2, an alcohol tank, an oven, and an oil bath. Experimental results show that the WFBG performance is affected significantly at extreme temperatures. The reflectivity of an acrylate coated WFBG decreases at cryogenic temperatures, whereas that of the bare WFBG is temperature independent. The reflectivity of the acrylate coated WFBG decreases from ~0.25% to

~0.15% in LH_2 immersion. Therefore, the bare WFBG should be used at cryogenic temperatures to ensure measurement accuracy and reliability. The sudden temperature change at high temperatures will result in transient and recoverable decreases in reflectivity. When the temperature is higher than 170°C, the grating erasure causes the irreversible decrease of reflectivity. Therefore, the WFBG can be used at cryogenic temperatures as low as −252.75°C, whereas they cannot be used for long-term application above 170°C. Finally, the temperature responses of Bragg wavelengths of WFBGs with different reflectivity are obtained, which show good linearity above −40°C. The WFBG with high reflectivity has better spectral SNR and measurement accuracy, and the WFBG with low reflectivity has better multiplexing capability. The optimum reflectivity in practical applications should be selected according to the requirements of measurement accuracy and multiplexing capability.

This work was supported by the National Natural Science Foundation of China (Nos. 61735011, 61675152, U1833104, and 61405159), the Natural Science Foundation of Tianjin City (No. 16JCQNJC02000), the National Key Research and Development Plan of China (No. 2016YFC0401902), and the open project of Key Laboratory of Opto-electronics Information Technology, Ministry of Education (No. 2018KFKT013).

References

1. S. J. Mihailov, Sensors (Basel) **12**, 1898 (2012).
2. J. Dai, M. Yang, Y. Chen, K. Cao, H. Liao, and P. Zhang, Opt. Express **19**, 6141 (2011).
3. J. Canning, Laser Photon. Rev. **2**, 275 (2008).
4. Y. Ran, F. R. Feng, Y. Z. Liang, L. Jin, and B. O. Guan, Opt. Lett. **40**, 5706 (2015).
5. F. R. Feng, Y. Ran, Y. Z. Liang, S. Gao, Y. H. Feng, L. Jin, and B. O. Guan, Opt. Lett. **41**, 2470 (2016).
6. D. Kinet, P. Mégret, K. W. Goossen, L. Qiu, D. Heider, and C. Caucheteur, Sensors (Basel) **14**, 7394 (2014).
7. Y. H. Pan, J. F. Jiang, W. Lu, H. Yang, K. Liu, S. Wang, and T. G. Liu, Chin. Opt. Lett. **15**, 070605 (2017).
8. W. H. Chung, H. Y. Tam, P. K. A. Wai, and A. Khandelwal, J. Lightwave Technol. **17**, 2709 (2005).
9. H. Y. Guo, F. Liu, Y. Q. Yuan, H. H. Yu, and M. Y. Yang, Opt. Express **23**, 4829 (2015).
10. C. M. Zhou, L. Qian, D. Fan, C. F. Cheng, and H. Y. Guo, Opt. Express **23**, 31484 (2015).
11. H. Guo, J. Tang, X. Li, Y. Zheng, H. Yu, and H. Yu, Chin. Opt. Lett. **11**, 030602 (2013).
12. P. Han, Z. Li, L. Chen, and X. Y. Bao, IEEE Photon. Technol. Lett. **29**, 1249 (2017).
13. T. Mizutani, N. Takeda, and H. Takeya, Struct. Health Monit. **5**, 205 (2006).
14. Z. S. Guo, J. Feng, and H. Wang, Cryogenics **52**, 457 (2012).
15. B. Zhang and M. Kahrizi, IEEE Sens. J. **7**, 586 (2007).
16. K. O. Hill and G. Meltz, J. Lightwave Technol. **15**, 1263 (1997).
17. P. Peterka, P. Koška, and J. Čtyroký, IEEE J. Sel. Top. Quant. **24**, 0902608 (2018).
18. Z. Chen, L. Yuan, G. Hefferman, and T. Wei, IEEE Photon. Technol. Lett. **27**, 1084 (2015).
19. M. L. Dockney, S. W. James, and R. P. Tatam, Meas. Sci. Technol. **7**, 445 (1996).
20. X. J. Fan, J. F. Jang, X. Z. Zhang, K. Liu, S. Wang, Y. N. Yang, and T. G. Liu, Opt. Express **26**, 22944 (2018).
21. L. A. Neely, V. Kochergin, E. M. See, and H. D. Robinson, J. Mater. Sci. **49**, 392 (2014).
22. J. Jiang, L. Song, T. Liu, J. Zhang, K. Liu, S. Wang, and T. G. Liu, Rev. Sci. Instrum. **84**, S387 (2013).
23. Y. Li, M. Yang, C. Liao, D. Wang, J. Lu, and P. Lu, J. Lightwave Technol. **29**, 1555 (2011).
24. K. Li, Z. Zhou, and A. Liu, Chin. Opt. Lett. **7**, 121 (2009).